Vibrational levels in the 86-neutron nucleus ^{150}Gd†

D. R. Haenni* and T. T. Sugihara

Cyclotron Institute, Texas A & M University, College Station, Texas 77843

(Received 26 October 1976)

The decay of 3.6-h ^{150}Tb to levels in ^{150}Gd has been studied by γ-ray and conversion-electron spectroscopy. A level scheme is proposed which accounts for all but 35 of the 256 γ rays assigned to this decay. Most of the low-lying levels in ^{150}Gd show a remarkably close correspondence with the predictions of the simple vibrator model. Possible candidates are observed for three-phonon quadrupole states and for the states coupling quadrupole and octupole phonons. The low-lying positive-parity levels can be adequately described by the phenomenological collective model of Gneuss and Greiner. The microscopic boson-expansion model of Kishimoto and Tamura, however, appears to predict ^{150}Gd to be more transitional than the data imply. Systematics of the 86-neutron isotones show increased stability at 64 protons. This can be correlated with the filling of the $g_{7/2}$ and $d_{5/2}$ spherical proton orbitals.

[RADIOACTIVITY ^{150}Tb [from ^{151}Eu(^{3}He, $4n$)], measured $T_{1/2}$, E_γ, E_{β^+}, I_γ, I_{ce}, γ-γ, and β^+-γ coin; deduced Q, $\log ft$. ^{150}Gd deduced levels, ICC, J, π. Enriched target, Ge(Li), and Si(Li) detectors.]

I. INTRODUCTION

The even-even 86-neutron nuclei are not well understood. Presumably they have spherical ground-state shapes and vibrational collective levels since they lie between the 82-neutron closed shell and the 88- to 90-neutron shape transition at the start of the deformed "rare earth" nuclei ($150<A<190$). Recent shell-model calculations[1-3] support the notion that many 86-neutron isotones have spherical ground-state shapes. Little experimental data have been accumulated concerning collective levels in these nuclei. Such data would be useful in obtaining additional insight into the systematics of nuclei around the shape transition and in providing examples of vibrational nuclei with more than 82 neutrons.

In a previous study of 5.8-min ^{150}Tb decay,[4] we noted that the energy spacing of the lowest 2^+, 4^+, and 6^+ levels in ^{150}Gd suggested a close correspondence with that expected for the vibrational model. Additional data on other low-spin multiphonon vibrational states are required to support this vibrational description of ^{150}Gd. Such states were not populated in the decay of the high-spin 5.8-min ^{150}Tb whose J^π is (9^+).[4] In an attempt to find these states we have studied in detail the decay of the low-spin 3.6-h ^{150}Tb.

While the work was in progress, Vylov *et al.*[5,6] reported that 96 γ rays were associated with 3.6-h ^{150}Tb decay. A scheme was proposed which accommodated 37 of these transitions among 17 levels. In general their experimental results are in good agreement with those obtained here, except as noted in Sec. II B. Levels in ^{150}Gd have also been observed in 5.8-min ^{150}Tb decay,[4,7,8] in (p,t) reactions,[9-11] and with in-beam γ-ray spectroscopy.[12-15] The results of these and previous 3.6-h ^{150}Tb decay studies[5,6,14,16,17] have recently been summarized.[18] Preliminary data from this work were included in the summary.

In the present study 256 γ rays are assigned to 3.6-h ^{150}Tb decay. The proposed decay scheme has 73 levels and accounts for all but 35 of the observed γ rays. Most of the positive- and negative-parity levels below 2 MeV can be qualitatively described in terms of the vibrational model that includes quadrupole and octuple vibrations. A more quantitative description of the positive-parity states is obtained with the phenomenological collective model of Gneuss and Greiner.[19] The energy spectrum is also compared with the predictions of the microscopic boson-expansion model of Kishimoto and Tamura.[20]

II. EXPERIMENTAL PROCEDURE AND RESULTS

A. Source preparation

Sources of 3.6-h ^{150}Tb were prepared via the ^{151}Eu(^{3}He, $4n$)^{150}Tb reaction with 35-MeV ^{3}He ions from the Texas A & M variable energy cyclotron. Targets consisted of 5 to 10 mg of Eu_2O_3 enriched to at least 95% in ^{151}Eu and were irradiated from 30 to 60 min with beam currents of 3 to 5 μA. Counting was not begun until one hour after bombardment. Thus the 5.8-min ^{150}Tb and 4.2-min ^{152}Tb activities were removed by decay. Significant amounts of 17-h ^{151}Tb and 18-h ^{152}Tb as well as smaller amounts of 4.1-h ^{149}Tb, 2.3-day ^{153}Tb, the several isomers of ^{154}Tb, and ^{24}Na were observed in the spectra from these sources.

Complications in the assignment of γ rays to

^{150}Tb decay arose primarily from the presence of ^{151}Tb and ^{152}Tb. Only the most intense rays from the other activities were visible in the γ-ray spectra. Since the half-life of ^{150}Tb is 3.6 ± 0.2 h, γ rays associated with ^{150}Tb could be separated from those associated with ^{151}Tb and ^{152}Tb decay on the basis of half-life. The decay data for ^{151}Tb by Vilskii *et al.*[21] and for ^{152}Tb by Zolnowski, Funk, and Mihelich[22] were used to analyze unresolved γ-ray multiplets consisting of an impurity line and a γ ray from ^{150}Tb.

B. Singles measurements

Singles γ-ray spectra were obtained with a 33-cm^3 Ge(Li) detector of resolution 1.8 keV full width at half maximum (FWHM) at 1.33 MeV. Standard modular electronics coupled with an on-line PDP-15/40 computer were used to acquire 8192-channel spectra. These spectra were analyzed with a modified version of the program SAMPO.[23] The calibration methods for energy and efficiency are described elsewhere.[24]

The energies and relative intensities of the γ rays assigned to 3.6-h ^{150}Tb are summarized in Table I. Included in the table are 67 weak transitions whose assignment to ^{150}Tb decay is tentative. Some of the relative intensities were deduced from γ-γ coincidence results while others have been corrected for unresolved components from either escape peaks or transitions from ^{151}Tb or ^{152}Tb decay.

Where they overlap, these results are in excellent agreement with those reported by Vylov *et al.*[5,6] except for the energies of γ rays above 4 MeV. In addition, the γ rays which Vylov *et al.*[5,6] reported at 1343.1, 2488.5, 2750.5, 3083.7, 3424.0, and 3604.0 keV are interpreted here as escape peaks.

Conversion-electron spectra were taken with two different spectrometer systems, both of which employ Si(Li) detectors to determine electron energies. The spectrum from 0.4 to 1.2 MeV was obtained with a cooled Si(Li) detector which directly views the source.[25] The second spectrometer system uses a broad-range, trochoidal-path steering magnet which selectively transports electrons from the source to a shielded and cooled Si(Li) detector. This system has been described in detail by Gono *et al.*[26] The spectrum from 0.8 to 1.5 MeV was obtained with this device.

The analysis of these spectra to obtain K-conversion coefficients is summarized in Table II. In some cases the observed electron intensity represents the sum of unresolved peaks. For three of these cases, one of the components was so small that it could be neglected. The rest were analyzed by assuming a multipolarity for all but one of the components. In general these results agree with those obtained by Vylov *et al.*[5,6] except for transitions between 560 and 570 keV and those at 1430.51 and 1453.6 keV.

C. Coincidence measurements

The Ge(Li) detector described above and a second counter of comparable size but poorer resolution were employed for a γ-γ-t coincidence measurement. The relative time t between more or less simultaneous events in both detectors was determined by conventional electronics using extrapolated leading-edge timing for the Ge(Li) detector signals. The data were recorded in an event-by-event mode on magnetic tape with an on-line PDP-15/40 computer.

The events were sorted into a $4096 \times 4096 \times$ two-channel spectrum using an IBM 7094 computer. The 4096-channel dimensions represent the energies of the coincident γ rays while the two-channel dimension separates prompt and random events. Coincidence spectra, corrected for random and Compton-background coincidences, were obtained by summing the appropriate portions of the $4096 \times 4096 \times$ two-channel spectrum.

The coincidence spectra were analyzed to obtain energies and intensities of the coincident γ rays. The detailed results of this analysis and a more complete description of the data reduction and analysis procedure may be found in Ref. 24.

The Q value for the decay of 3.6-h ^{150}Tb was determined from a β^+-γ coincidence measurement. This experiment was essentially the same as the γ-γ-t coincidence measurement except that the second detector was a cylindrical NE102 scintillator 4 cm long and 5 cm in diameter. The data were corrected for γ-γ coincidences from a measurement in which a 4.3 g/cm^2 Cu absorber was placed between the source and the scintillator. This spectrum, suitably normalized, was subtracted from the measurement without absorber. Corrections for summing with annihilation radiation were made by calibrating the scintillator for energy with radioactive sources of known β^+ energy.

The spectrum of β^+ particles populating a particular level was obtained by summing the β^+ spectra gated by the γ rays depopulating that level. End-point energies, determined from Kurie plots[28] and $\log ft$ values[29] for these β transitions, are summarized in Table III.

Population of the ^{150}Gd ground state was indicated in the β^+ spectrum gated by 511-keV annihilation radiation. The end-point energy of the highest β^+ group in this spectrum was ~625 keV higher than that of the group observed to feed the 638.05-

TABLE I. Energies and intensities of γ rays in 3.6-h ^{150}Tb decay.

Energy (keV)	Relative intensity	Placement[a]
128.0(3)[b]	5(2)	2956→2828
		[2687→2559]
153.9(3)	10(2)	1288→1134
		[4265→4111]
222.8(3)[b]	9(2)	
275.6(3)[b]	8(2)	
300.4(5)[b]	9(3)	4322→4022
303.1(5)[b]	5(2)	
330.1(2)	15(3)	2985→2654
		[3840→3510]
338.2(2)	25(5)	2326→1988
378.8(5)[c]	20(10)	2326→1947
384.1(3)	60(10)	1518→1134
385.5(5)[c]	10(5)[d]	1592→1207
411.7(4)	115(10)[d]	1700→1288
412.4(2)[e]	~10	1701→1288
425.9(5)[c]	50(25)	2985→2559
437.1(1)	130(5)	1955→1518
491.7(2)	25(5)[d]	2084→1592
496.30(10)	2 060(40)[d]	1134→638
525.0(2)	80(10)	1955→1430
526.0(3)	17(7)[d]	1814→1288
557.5(1)	50(5)[d]	1988→1430
565.7(1)	155(10)	1700→1134
566.7(2)	20(5)	1701→1134
569.1(1)	350(10)[d]	1207→638
573.4(2)	45(5)	2091→1518
602.8(2)	30(5)[d]	2687→2084
609.3(3)[b]	10(5)	2564→1955
		[3035→2426]
638.05(10)	≡10 000	638→0
649.5(5)[c]	40(20)[d]	2080→1430
650.4(2)	560(20)[d]	1288→638
661.0(3)	≤30[d]	2091→1430
666.3(2)[b]	13(5)[d]	2654→1988
699.4(2)	45(5)[d]	1988→1288
743.8(2)	20(5)	2262→1518
746.6(2)	10(3)	2956→2209
748.3(2)	65(5)[d]	1955→1207
772.6(2)	30(5)[d]	2365→1592
779.0(5)	40(5)[d]	2209→1430
791.1(5)	35(15)	2080→1288
792.5(3)	610(20)	1430→638
808(1)[b]	10(4)[d]	2326→1518
813.1(3)	95(20)[d]	1947→1134
821.1(2)	190(10)[d]	1955→1134
831.5(2)	15(5)[d]	2786→1955
880.3(1)	420(10)[d]	1518→638
884.6(2)	45(10)	2091→1207
895.9(3)	30(5)	2326→1430
950.0(2)	125(10)	2084→1134
952.0(5)	10(5)	3035→2084
954.5(3)	160(10)[d]	1592→638
957.4(2)	110(10)	2091→1134
968.4(2)	20(5)	2956→1988
978.1(3)	15(5)	2408→1430
995.5(3)	20(5)[d]	2426→1430
997.7(4)	12(3)	2985→1988
1001.0(3)	15(3)	2956→1955
1003.8(3)	12(2)	2521→1518
		[3083→2080]
		[4379→3375]
1045.72(10)	175(10)	2180→1134
1061.9(5)[b]	15(7)	1700→638
1075.3(1)	85(5)	2209→1134
1091.2(3)	25(10)	2521→1430
1094.4(3)	30(5)[d]	2687→1592
1120.1(3)	20(5)	2408→1288
1128.2(4)	25(5)	2828→1700
1134.3(3)	15(5)	2564→1430
1135.3(5)[c]	15(5)	3344→2209
1157.7(5)	30(10)[d]	2365→1207
1168.7(2)	60(5)[d]	2687→1518
1176.0(2)	65(5)[d]	1814→638
1191.1(4)	15(5)[d]	4176→2984
1224.2(5)	12(4)	2654→1430
		[4344→3119]
1233.0(4)	25(5)	2521→1288
1253.1(3)	12(3)	2845→1592
		[3344→2091]
1256.6(5)[b]	~7	2687→1430
		[2956→1700]
1274.6(2)	25(5)[d]	2408→1134
1291.65(10)	225(10)[d]	2426→1134
1317.6(3)	50(10)[d]	1955→638
1350.1(5)	150(50)	1988→638
1351.9(5)	35(15)[d]	2559→1207
1356.1(3)	20(5)[d]	2786→1430
1387.0(4)	15(5)	2521→1134
1392.1(3)[b]	5(2)[d]	2985→1592
1415.0(2)	40(10)[d]	2845→1430
1430.51(10)	300(20)[d]	1430→0
1430.5(3)[c]	40(20)[d]	2564→1134
1442.0(5)	10(3)[d]	2080→638
1443.6(3)	55(5)[d]	3035→1592
1446.2(3)	70(5)[d]	2084→638
1453.62(10)	500(15)	2091→638
1466.6(4)	10(2)	2755→1288
1493.0(5)	15(5)	2627→1134
1516.5(5)[c]	45(10)[d]	3035→1518
1518.5(2)	320(10)[d]	1518→0
1525.8(1)	55(5)	2956→1430
1542.0(2)	55(5)	2180→638
1552.7(2)	15(5)	2687→1134
		[4207→2564]
1554.7(2)	25(5)	2985→1430
1564.2(2)	15(5)	3378→1814
1571.3(3)[b]	5(2)[d]	2209→638
1580.0(3)[b]	10(5)[d]	2786→1207
		[4145→2564]
1592.7(1)	225(10)[d]	1592→0
1605.6(5)	15(5)[d]	3035→1430
1615.4(4)	15(5)	
1620.7(3)	20(5)	2755→1134
1624.4(3)	40(10)[d]	2262→638
1638.6(10)[b]	10(5)[d]	2845→1207
1652.7(3)	20(10)	2786→1134
1660.2(2)	20(5)[d]	3178→1518

TABLE I. (*Continued*)

Energy (keV)	Relative intensity	Placement [a]
1670.5(10) [b]	30(10) [d]	3658 → 1988
1688.2(4)	45(10)	2326 → 638
1688.8(4) [c]	20(5)	3119 → 1430
1703.1(4) [b]	10(5)	3658 → 1955
1726.9(4)	30(5) [d]	2365 → 638
1752.2(5)	15(5) [d]	3344 → 1592
1770.8(2)	75(5) [d]	2408 → 638
1778.0(5) [c]	15(8) [d]	2985 → 1207
1778.8(5)	70(10) [d]	2416 → 638
1788.13(10)	225(10) [d]	2426 → 638
1796.6(2)	25(5) [d]	4207 → 2408
1811.8(5) [b]	10(5) [d]	4176 → 2365
1831.9(4)	15(5)	4258 → 2426
1884.0(3)	25(10) [d]	2521 → 638
1900.6(10)	70(30) [d]	3035 → 1134
1914.4(2)	40(20) [d]	3344 → 1430
1926.8(3)	20(5)	2564 → 638
1949.3(3)	25(5) [d]	3083 → 1134
1955.7(3) [b]	~5 [d]	1955 → 0
		[4165 → 2209]
1985.1(2)	15(5) [d]	3119 → 1134
2016.6(3)	130(20) [d]	2654 → 638
2040.6(3)	50(5) [d]	2678 → 638
2044.3(3)	10(2) [d]	3178 → 1134
2056.4(5)	15(5)	3344 → 1288
2091.7(3)	200(20)	2091 → 0
2117.0(3)	50(5) [d]	2755 → 638
2137.2(4) [b]	5(2)	3344 → 1207
		[4545 → 2408]
2148.7(3)	140(5) [d]	2786 → 638
2169.3(5) [b]	15(3) [d]	4379 → 2209
2173.4(5)	20(5)	3460 → 1288
2180.0(3)	50(5) [d]	2180 → 0
		[4545 → 2365]
2190.3(5) [b]	8(2)	2828 → 638
2194.9(5)	40(5) [d]	3329 → 1134
2201.3(3) [b]	10(3)	
2207.8(3)	140(10)	2845 → 638
2230.0(5) [b]	10(3) [d]	4322 → 2091
		[4314 → 2084]
2233.7(5) [b]	8(2)	4314 → 2080
2241.3(4) [b]	20(10) [d]	3375 → 1134
2258.7(5) [b]	4(2) [d]	
2263.0(4) [b]	10(5) [d]	4344 → 2080
2283.5(5) [b]	5(3)	4545 → 2262
2296.7(5) [b]	5(2) [d]	3726 → 1430
		[4111 → 1814]
2318.2(3)	55(10)	2956 → 638
2329.6(5) [b]	5(2) [d]	
2347.2(3)	25(5) [d]	2985 → 638
2365.1(3)	120(10) [d]	2365 → 0
2376.5(4) [b]	13(5) [d]	3510 → 1134
2396.5(4)	80(5) [d]	3035 → 638
2410.0(3)	45(10)	3840 → 1430
2426.3(3)	125(5) [d]	2426 → 0
2449.8(5) [b]	3(1) [d]	4406 → 1955
		[4530 → 2080]
2460.7(4)	11(3)	4545 → 2084
2494.6(4)	25(5) [d]	
2498(1) [b]	10(5) [d]	4446 → 1947
2532.3(4) [b]	10(5) [d]	
2539.5(3)	65(10) [d]	3178 → 638
2552.3(5) [b]	6(2) [d]	3840 → 1288
		[4145 → 1592]
2558.9(3)	30(5)	2559 → 0
2565.5(5) [b]	7(3)	4745 → 2180
2592.1(3)	35(5) [d]	3726 → 1134
2614.4(4) [b]	10(2) [d]	4207 → 1592
2622.1(5) [b]	5(2) [d]	4322 → 1700
		[3829 → 1207]
2661.0(3)	20(5)	4745 → 2084
2669.0(3)	15(5)	
2678.6(5)	15(5)	2678 → 0
		[4379 → 1700]
2690.5(5) [b]	10(3) [d]	3329 → 638
2706.6(4)	40(5) [d]	3344 → 638
2737.5(4)	40(5)	3375 → 638
2740.0(2)	30(10) [d]	3378 → 638
2774.7(3)	12(3)	4207 → 1430
2808.0(3) [b]	8(2) [d]	
2841.3(5) [b]	5(2) [d]	
2845.6(3)	25(5) [d]	2845 → 0
		[4545 → 1700]
2872.4(3)	30(5) [d]	3510 → 638
2876.6(3)	15(5) [d]	4165 → 1288
2895.0(5) [b]	4(2) [d]	
2913.4(4)	7(3) [d]	4344 → 1430
2936.0(4) [b]	7(2) [d]	4530 → 1592
2952.7(4)	8(2) [d]	4545 → 1592
2976.2(5) [b]	5(2) [d]	4265 → 1288
		[4111 → 1134]
2984.4(5)	50(10) [d]	2985 → 0
2993.4(5)	8(3) [d]	
3009.9(4)	6(3)	4146 → 1134
3024.5(5)	5(2) [d]	
3034.0(10)	15(5)	4322 → 1288
3035.5(10)	25(5)	3035 → 0
3042.6(4) [b]	10(5) [d]	4176 → 1134
3096.3(4)	15(5) [d]	
3102.6(4)	9(1)	4237 → 1134
3123.9(4) [b]	10(2) [d]	4258 → 1134
3130.5(15)	4(2) [d]	4265 → 1134
3134.7(4)	15(5) [d]	
3152.4(4)	9(2)	4745 → 1592
3168.3(4)	8(2)	
3191.6(4)	6(2)	3829 → 638
3197.7(4)	6(2)	4406 → 1207
3202.5(4)	10(2)	3840 → 638
3238(1)	7(2)	4446 → 1207
3262.3(4) [b]	7(3) [d]	
3315.0(5) [b]	4(2)	4745 → 1430
3327.8(5)	8(2) [d]	
3344.7(5)	5(1)	3344 → 0
3352.3(5)	5(1)	
3374(1) [b]	5(2) [d]	
3383.6(5) [b]	8(4) [d]	4022 → 638
3389.8(5) [b]	5(2)	4524 → 1134
3411.3(5) [b]	4(2) [d]	4545 → 1134

TABLE I. (*Continued*)

Energy (keV)	Relative intensity	Placement[a]	Energy (keV)	Relative intensity	Placement[a]
3440.8(5)	6(2)		3885(2)[b]	2(1)	4524→638
3448.1(5)[b]	2(1)		3927(2)[b]	4(2)	
3460(1)[b]	4(2)	3460→0	4022(2)	5(2)[d]	4022→0
3473(1)	5(1)	4111→638	4107(2)	15(5)	4745→638
3484.5(5)	7(2)		4112(2)	10(3)	4111→0
3489.7(5)	7(2)		4146(2)	3(1)	4146→0
3509.8(5)	8(3)[d]	3510→0	4164(2)	2(1)	4165→0
3523(1)	9(1)		4206(1)	9(2)	4207→0
3551(2)[b]	5(3)		4236(2)[b]	~1	4237→0
3555(2)[b]	4(2)		4246(1)	6(2)	4246→0
3571(1)[b]	4(2)[d]	4207→638	4257(2)	2(1)	4258→0
3658.2(5)	14(2)	3658→0	4265(2)	5(1)	4265→0
3675(2)	8(2)	4314→638	4284(2)	2(1)	4284→0
3685(2)[b]	5(2)	4322→638	4290(1)	14(4)	4290→0
3735(2)[b]	10(4)[d]		4314(1)	4(1)	4314→0
3769(2)	5(2)	4406→638	4322(1)	6(1)	4322→0
3774(2)[b]	5(2)[d]		4344(2)[b]	~1	4344→0
3817(2)[b]	3(2)		4379(2)[b]	~1	4379→0
3829(2)	5(2)	3829→0	4406(2)	7(2)	4406→0
3836(2)	7(2)		4446(1)	11(2)	4446→0
3846(2)[b]	3(2)		4531(2)[b]	~1	4530→0

[a]Brackets indicate alternate placements in the level scheme.
[b]Tentatively assigned to 3.6-h ^{150}Tb from γ-ray singles measurements.
[c]Assigned to 3.6-h ^{150}Tb from γ-γ coincidence results.
[d]Intensity corrected for unresolved γ ray from ^{151,152}Tb or escape peak.
[e]Existence of γ ray inferred from observation of 566.7-keV γ ray and 5.8-min ^{150}Tb decay scheme (Ref. 4).

keV level. Furthermore, the end-point energy of this group is higher than the highest energy β^+ group among the impurities known to be present in the ^{150}Tb sources.

III. DECAY SCHEME

The proposed decay scheme for 3.6-h ^{150}Tb contains 73 levels, 15 of which are considered tentative. The data are presented in tabular form, Table IV, because of the complexity and amount of information to be summarized. Most of the transitions are placed in the scheme using either γ-γ coincidence results or energy sums and differences. Transitions with energies above 4130 keV are assumed to feed the ground state since any other placement would be inconsistent with the measured Q value. The basis for placing each transition in the scheme is indicated in Table IV. Most of the levels were constructed in a straightfoward manner from the level scheme found in 5.8-min ^{150}Tb decay[4] and the γ-γ coincidence data in the present work. For this reason detailed arguments for the establishment of each level are not given.

Transition multipolarities and decay patterns were used to deduce J^π values. Where conversion data were unavailable, transitions were assumed to be $E1$, $M1$, or $E2$. In addition to the results listed in Table II, the multipolarities determined by Vylov *et al.*[5,6] for the 813.1- and 821.1-keV transitions [($E2$) and $E1$, respectively] and by Kewley *et al.*[13] for the 1176.0- and 1350.1-keV transitions ($E1$ and $E2$, respectively) have been used in making J^π assignments. The J^π of the 1592.7-keV level was chosen to be consistent with the $E1$ multipolarity assigned to the 954.5-keV transition. Vylov *et al.*[5,6] assign the multipolarity of the 1592.7-keV transition as $M1$. Other differences between the present conversion-electron results and those of Vylov *et al.*[5,6] have already been noted.

The amount of β-decay feeding each level was calculated from transition intensity balances and the absolute intensity of the 638.05-keV γ ray as reported by Vylov *et al.*[5,6] As indicated in Table IV, most of the levels receive $<1\%$ of the β-decay intensity. In may cases this is less than the amount of unplaced γ-ray intensity which could feed the level. Logf_0t values were given in Table III for the transitions observed in the β^+-γ coincidence experiment. For the rest of the levels the logf_0t and logf_1t values are consistent with the transitions being allowed, first forbidden or, in

TABLE II. *K*-conversion coefficients for transitions in 3.6-h ^{150}Tb decay.

E_γ (keV)	I_{ce}	α_K (units 10^{-4}) Exp. [a]	Theo. [b] $E1/E2/M1$	Multipolarity
411.7 + 412.3 [c]	3.8(8)	320(70)	62/190/460	$M1$
437.1	3.4(3)	260(30)	55/160/310	$M1+E2$
496.30	8.7(10)	42(15)	41/120/220	$E1$
525.0 + 526.0 [c]	2.1(4)	220(20)	36/100/190	($M1$)
557.5	0.44(5)	88(13)	32/87/170	$E2$
565.7 + 566.7 [e] + 569.1 [e]	3.5(7)	30(50)	31/82/160	($E1$)
573.4	0.76(16)	170(40)	30/81/160	$M1$
638.05	≡62.4	≡62.4	62.4	$E2$ [d]
649.5 [f] + 650.4	3.3(4)	55(7)	23/60/110	$E2$
791.1 [f] + 792.3	2.3(3)	36(4)	15/38/70	$E2$
880.3 + 884.6 [e]	2.3(3)	51(5)	12/30/54	$M1$
950.0	0.51(14)	41(12)	11/26/45	($M1$)
952.0	0.04(2)	40(30)	11/26/45	
954.5	0.12(3)	8(3)	11/26/45	$E1$
957.4	0.12(3)	11(3)	11/26/46	$E1$
1045.72	0.21(11)	12(6)	9/21/36	$E1$
1075.3	0.26(4)	31(5)	9/20/33	$M1$
1207.2	3.2(4)			$E0$
1233.0	0.013(3)	5(2)	7/15/24	$E1$
1274.6	0.018(5)	7(2)	6/14/22	$E1$
1291.65	0.14(2)	6(1)	6/14/22	$E1$
1415.0	0.03(1)	7(3)	5/12/18	$E1$
1430.5 [f] + 1430.51	0.41(6)	12(2)	5/12/17	$E2$
1453.62	0.74(10)	15(2)	5/11/17	($M1$)

[a] The necessary γ-ray data have been taken from Table I.
[b] Reference 27.
[c] Assumed to be $E1$ to resolve multiple peak.
[d] Measured to be $E2$ (Ref. 13); used to normalize electron and γ-ray data.
[e] Assumed to be $E2$ to resolve multiple peak.
[f] This transition is very weak.

TABLE III. Endpoint energies and log*ft* values for β^+ populating particular levels in ^{150}Gd from 3.6-h ^{150}Tb decay.

Level energy (keV)	β^+ endpoint energy (keV)	Q (keV)	$I(\beta^+, \mathrm{EC})$ [a] (%)	$\log f_0 t$ [b]	$\log f_1 t$ [b]
g.s.	3730(120) [c]	4752(120)	15.4(40)	7.8	9.5
638.05	3105(100)	4765(100)	25.1(30)	7.2	8.8
1134.35	2580(120)	4736(120)	2.8(6)	8.0	9.5
1288.4	2500(155)	4811(155)	1.5(3)	8.2	9.7
1518.5	2170(100)	4711(100)	3.3(4)	7.8	9.3
1700.1	2060(100)	4782(100)	1.8(3)	7.9	9.4
1955.0	1805(95)	4783(95)	3.4(4)	7.5	8.9
2084.4	1665(110)	4771(110)	1.1(2)	8.0	9.4
2091.7	1655(80)	4769(80)	6.6(9)	7.2	8.6
2180.1	1590(110)	4792(110)	2.0(3)	7.7	9.1
	Average	4765(35)			

[a] Intensity of β-decay branch, from Table IV.
[b] Calculated using tables in Ref. 29.
[c] See text for details of assigning β^+ branch to ground state.

TABLE IV. Decay scheme for 3.6-h ^{150}Tb.

Level no.	Level energy (keV)	J^π	$I(\beta^+, \mathrm{EC})$ [a] (%)	Depopulating transitions [b]
1	0.0	0^+	15.4(40)	None
2	638.05(10)	2^+	25.1(30)	638.05[1]*A*
3	1134.35(15)	3^-	2.8(6)	496.30[2]*A*
4	1207.2(2)	0^+	0.8(2)	569.1[2]*A*, 1207.2[1]*B*
5	1288.4(2)	4^+	1.5(3)	153.9[3]*B*, 650.4[2]*A*
6	1430.5(2)	$(1, 2)^+$	1.9(4)	792.5[2]*A*, 1430.51[1]*A*
7	1518.5(2)	2^+	3.3(4)	384.1[3]*A*, 880.3[2]*A*, 1518.5[1]*A*
8	1592.7(2)	1^-	1.7(3)	385.5[4]*A*, 954.5[2]*A*, 1592.7[1]*A*
9	1700.1(2)	$(3, 4)^+$	1.8(3)	411.7[5]*A*, 565.7[3]*A*, 1061.9[2]*A*
10	1700.9(2) [c]	5^-	0.2(1)	412.3[5]*B*, 566.7[3]*B*
11	1814.3(3)	3^-	0.5(1)	526.0[5]*A*, 1176.0[2]*A*
12	1947.5(3)	$(2, 3, 4^{d})^-$	0.5(2)	813.1[3]*A*
13	1955.6(2)	2^+	3.4(4)	437.1[7]*A*, 525.0[6]*A*, 748.3[4]*A*, 821.1[3]*A*, 1317.7[2]*A*, 1955.7[1]*B*
14	1988.0(3)	$(2, 3, 4^{e})^+$	1.0(4)	557.5[6]*A*, 699.4[5]*A*, 1350.1[2]*A*
15	2080.0(5)	$(2^+, 3^\pm, 4^+)^{f}$	0.5(2)	649.5[6]*A*, 791.1[5]*A*, 1442.0[2]*A*
16	2084.4(2)	$(2, 3)^-$	1.1(2)	491.7[8]*A*, 950.0[3]*A*, 1446.2[2]*A*
17	2091.7(2)	2^+	6.6(9)	573.4[7]*A*, 661.0[6]*B*, 884.6[4]*A*, 957.4[3]*A*, 1453.62[2]*A*, 2071.7[1]*A*
18	2180.1(2)	2^+	2.0(3)	1045.72[3]*A*, 1542.0[2]*A*, 2180.1[1]*B*
19	2209.5(3)	$(2, 3^{e})^-$	0.7(1)	779.0[6]*A*, 1075.3[3]*A*, 1571.3[2]*A*
20	2262.4(3)		0.4(1)	743.8[7]*A*, 1624.4[2]*A*
21	2326.3(5)		0.9(2)	338.2[14]*A*, 378.8[12]*A*, 808[7]*A*, 895.9[6]*A*, 1688.2[2]*A*
22	2365.1(3)	$(1^\pm, 2^+)$	1.4(2)	777.6[8]*A*, 1157.7[4]*A*, 1726.9[2]*A*, 2365.1[1]*A*
23	2408.8(3)	$(2, 3, 4^{e})^+$	0.8(1)	978.1[6]*A*, 1120.1[5]*B*, 1274.6[3]*A*, 1770.8[2]*A*
24	2416.9(5) [g]		0.5(1)	1778.8[2]*A*
25	2426.1(3)	2^+	4.2(5)	995.5[6]*A*, 1291.65[3]*A*, 1788.13[2]*A*, 2426.3[1]*B*
26	2521.8(5)	$(2^+, 3^\pm, 4^+)^{f}$	0.7(1)	1003.8[7]*B*, 1091.2[6]*A*, 1233.0[5]*A*, 1387.0[3]*A*, 1884.0[2]*A*
27	2559.0(3)	$(1^\pm, 2^+)$	0.1(2)	1351.9[4]*A*, 2558.9[1]*B*
28	2564.9(3)		0.5(1)	609.3[12]*B*, 1134.3[6]*A*, 1430.5[3]*A*, 1926.8[2]*A*
29	2627.4(5) [g]		0.11(4)	1493.1[3]*A*
30	2654.5(3)		1.1(2)	666.3[14]*A*, 1224.1[6]*B*, 2016.5[2]*A*
31	2678.6(3)	$(1^\pm, 2^+)$	0.5(1)	2040.6[2]*A*, 2678.6[1]*B*
32	2687.2(3)	$(1^-, 2^\pm, 3^-)$	1.0(2)	128.0[27]*D*, 602.2[16]*A*, 1094.4[8]*A*, 1168.7[7]*A* 1256.6[6]*B*, 1552.7[3]*B*
33	2755.1(3)	$(2^+, 3^\pm, 4^+)$	0.6(1)	1466.6[5]*A*, 1620.7[3]*A*, 2117.0[2]*A*
34	2786.9(4)	$(1^-, 2^+)$	1.5(2)	831.5[13]*A*, 1356.1[6]*A*, 1580.0[4]*B*, 1652.7[3]*A*, 2148.7[2]*A*
35	2828.4(5)		0.20(4)	1128.2[9]*A*, 2190.3[2]*B*
36	2845.8(4)	$(1^\pm, 2^+)$	1.6(2)	1253.1[8]*B*, 1415.0[6]*A*, 1638.6[4]*A*, 2207.7[2]*A*, 2845.6[1]*B*
37	2956.4(3)		1.2(2)	128.0[35]*B*, 746.6[19]*B*, 968.4[14]*A*, 1001.0[13]*A*, 1525.8[6]*A*, 2318.2[2]*A*
38	2985.0(6)		1.3(3)	330.1[28]*B*, 425.9[27]*A*, 997.7[14]*A*, 1392.1[8]*A*, 1554.7[6]*A*, 1778.0[4]*A*, 2347.1[2]*A*, 2984.4[1]*B*
39	3035.6(10)	$(1^-, 2^+)$	2.2(4)	609.3[25]*D*, 952.0[16]*A*, 1443.6[8]*A*, 1516.5[7]*A*, 1605.6[6]*A*, 1900.6[3]*A*, 2396.5[2]*A*, 3035.5[1]*B*
40	3083.7(3) [g]		0.18(4)	1003.8[15]*D*, 1949.3[3]*A*
41	3119.3(3)		0.25(6)	1688.8[6]*A*, 1985.0[3]*A*
42	3178.3(6)		0.7(1)	1660.2[7]*A*, 2044.3[3]*A*, 2539.5[2]*A*
43	3329.0(5)		0.4(1)	2194.9[3]*A*, 2690.5[2]*B*
44	3344.8(5)	(2^+)	1.0(2)	1135.0[19]*A*, 1253.1[17]*D*, 1752.2[8]*A*, 1914.4[6]*A*, 2056.4[5]*A*, 2137.1[4]*B*, 2706.6[2]*A*, 3344.7[1]*B*
45	3375.7(3)		0.4(1)	2241.3[3]*A*, 2737.5[2]*A*
46	3378.3(5)		0.3(1)	1564.2[1]*A*, 2740.0[2]*B*
47	3961(1)	(2^+)	0.17(5)	2173.4[5]*A*, 3460[1]*B*
48	3510(1)	$(1^-, 2^+)$	0.4(1)	2376.5[3]*A*, 2872.4[2]*A*, 3509.5[1]*B*
49	3658.5(5) [g]		0.4(1)	1670.5[14]*B*, 1703.1[13]*B*, 3658.2[1]*B*
50	3726.9(6)		0.3(1)	2296.7[6]*B*, 2592.1[3]*A*
51	3829.7(10) [g]	$(1^\pm, 2^+)$	0.08(2)	2622.1[4]*D*, 3191.6[2]*B*, 3829[1]*B*
52	3840.6(5)		0.4(1)	330.1[48]*D*, 2410.0[6]*A*, 2552.3[5]*B*, 3202.5[2]*B*

TABLE IV. (*Continued*)

Level no.	Level energy (keV)	J^{π}	$I(\beta^{+}, \mathrm{EC})$[a] (%)	Depopulating transitions[b]
53	4022(1)[g]	$(1^{\pm}, 2^{+})$	0.06(3)	3383.6[2]*B*, 4022[1]*B*
54	4111(1)[g]	$(1^{\pm}, 2^{+})$	0.11(3)	2296.7[11]*D*, 2976.2[3]*D*, 3473[2]*B*, 4111[1]*B*
55	4145(1)[g]	$(1^{-}, 2^{+})$	0.06(2)	1580.0[28]*D*, 2552.3[3]*D*, 3009.9[3]*B*, 4146[1]*C*
56	4165(1)	(2^{+})	0.12(4)	1955.7[19]*D*, 2876.6[5]*A*, 4164[1]*C*
57	4176.6(5)		0.3(1)	1191.1[38]*A*, 1811.8[22]*B*, 3042.6[3]*B*
58	4207(2)	$(1^{\pm}, 2^{+})$	0.4(1)	1552.7[30]*D*, 1796.6[23]*B*, 2614.4[8]*B*, 2774.7[6]*B*, 3571[2]*B*, 4207[1]*C*
59	4237(1)[g]	$(1^{-}, 2^{+})$	0.07(2)	3102.6[3]*B*, 4236[1]*C*
60	4246(2)[g]	$(1^{\pm}, 2^{+})$	0.04(2)	4246[1]*C*
61	4258(1)	$(1^{-}, 2^{+})$	0.19(6)	1831.9[25]*B*, 3123.9[3]*B*, 4257[1]*C*
62	4265(1)	(2^{+})	0.12(3)	153.9[54]*D*, 2976.2[5]*B*, 3130.5[3]*B*, 4265[1]*C*
63	4284(2)[g]	$(1^{\pm}, 2^{+})$	0.01(1)	4284[1]*C*
64	4290(2)[g]	$(1^{\pm}, 2^{+})$	0.10(3)	4290[1]*C*
65	4314(1)		0.14(3)	2240.0[16]*D*, 2233.7[15]*B*, 3675[2]*B*, 4314[1]*C*
66	4322(1)	(2^{+})	0.4(1)	300.4[53]*B*, 2230.0[17]*B*, 2622.1[9]*B*, 3034.0[5]*B*, 3685[2]*B*, 4322[1]*C*
67	4344(1)	$(1^{\pm}, 2^{+})$	0.13(5)	1224.2[41]*D*, 2263.1[15]*B*, 2913.4[6]*B*, 4344[1]*C*
68	4379(1)[g]	$(1^{\pm}, 2^{+})$	0.11(3)	1003.9[45]*D*, 2169.3[19]*B*, 2678.6[9]*D*, 4379[1]*C*
69	4406(1)	$(1^{\pm}, 2^{+})$	0.13(3)	2449.8[13]*B*, 3197.7[4]*B*, 3769.2[2]*B*, 4406[1]*C*
70	4446(1)		0.20(5)	2498.0[12]*B*, 3238[4]*B*, 4446[1]*C*
71	4524(1)[g]		0.05(2)	3389.8[3]*B*, 3885[2]*B*
72	4530(2)[g]	$(1^{\pm}, 2^{+})$	0.06(2)	2449.8[15]*D*, 2936.0[8]*B*, 4531[1]*C*
73	4545.5(10)		0.20(4)	2137.2[23]*D*, 2180.0[22]*D*, 2283.3[20]*B*, 2460.7[16]*B*, 2845.6[9]*D*, 2952.7[8]*B*, 3411.3[3]*B*
74	4745.5(10)		0.4(1)	2565.5[18]*B*, 2661.0[16]*B*, 3152.4[8]*B*, 3315.0[6]*B*, 4107[2]*B*

[a] Calculated assuming 72(9)% of the decays result in a 638.05-keV γ ray.

[b] Number in brackets indicates the level fed by the transition. Letters indicate placement by *A*, coincidence data; *B*, energy sums; *C*, placed feeding the ground state in order to be consistent with the measured *Q* value; *D*, alternate placements for transitions placed by energy sums.

[c] The existence of this level is well established from 5.8-min ^{150}Tb decay (Ref. 4). Evidence for its population in 3.6-h ^{150}Tb decay is weak.

[d] Allowed only if there is no direct β feeding to this level.

[e] Allowed only if 1430.5-keV level is 2^{+}.

[f] 3^{-} and 4^{+} allowed only if 1430.5-keV level is 2^{+}.

[g] Tentative level.

some cases, first-forbidden unique.[30]

The β^{+}-γ coincidence measurement indicates that the 0^{+} ground state and the 4^{+} level at 1288.4 keV are directly populated by β decay. The $\log f_1 t$ values for these transitions are consistent with their being first-forbidden unique.[30] Therefore, the J^{π} of the 3.6-h ^{150}Tb state is most likely 2^{-}. If this assignment is correct, then one would not expect direct β feeding to either the 1700.9-keV 5^{-} level or the 1947.5-keV level if it is 4^{-}.

The levels in ^{150}Gd proposed in previous ^{150}Tb decay studies[5,6,14,16,17] are in general confirmed by the present results. The placement of a few transitions and some J^{π} assignments have been changed. The only other difference worth noting concerns the two levels at 1700 keV. Some confusion has resulted since a distinction between them has not been made in previous work. The 1700.9-keV 5^{-} level is observed in in-beam studies[13-15] and in 5.8-min ^{150}Tb decay.[4,7,8] It decays to the 1288.4-keV 4^{+} and 1134.35-keV 3^{-} levels via 412.3-keV *E*1 and 566.52-keV *E*2 transitions, respectively.[15] In 3.6-h ^{150}Tb decay a 1700.3-keV $(3,4)^{+}$ level is directly populated by β decay. This level is depopulated by a 411.7-keV *M*1 transition to the 1288.4-keV level and a 565.7-keV (*E*1) transition to the 1134.35-keV level. Experimental evidence that the 566.52- and 565.7-keV transitions are not the same is seen in Fig. 1 where γ-ray spectra obtained at the same gain for 3.6-h and 5.8-min ^{150}Tb are compared. The observation of a weak (566.7 ± 0.3)-keV peak as a shoulder on the 565.7-keV peak in the spectrum for 3.6-h ^{150}Tb decay provides the only evidence for the population of the 1700.9-keV level in the decay of 3.6-h ^{150}Tb.

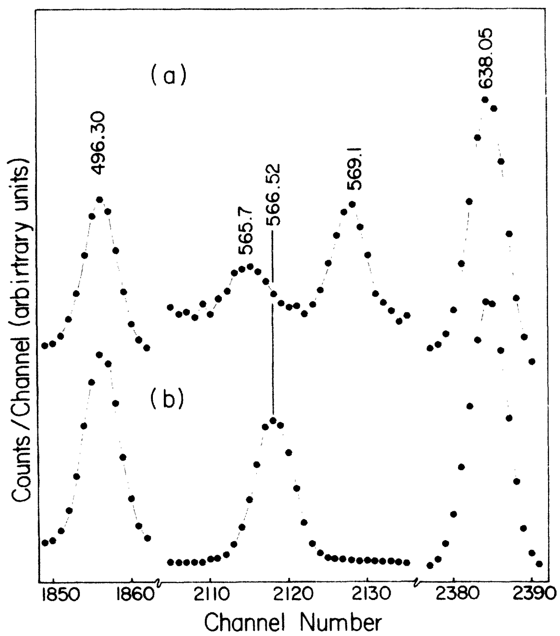

FIG. 1. γ-ray spectra from (a) 3.6-h and (b) 5.8-min ^{150}Tb decay. The gain in the two spectra is the same. The difference in energy between the peaks at 565.7 $\pm$ 0.1 and 566.52 $\pm$0.10 keV is clearly observed.

IV. DISCUSSION

A. Qualitative description of low-lying levels

The low-lying levels in ^{150}Gd are summarized in the level scheme in Fig. 2. Levels populated in the decay[4] of 5.8-min ^{150}Tb and those observed in (p,t) reaction studies[9-11] are also included. An in-beam γ-ray study[15] using the $(\alpha, 4n)$ reaction found no additional states below 2100 keV. Of the 17 levels below 2100 keV, 15 can be described in terms of the vibrational model. The remaining two levels appear to have quasiparticle character.

A possible correspondence between the experimental levels and those predicted by the vibrational model[31] is indicated on the left in Fig. 2. The one-phonon energies of the quadrupole and octupole oscillators were assumed to be 638 and 1134 keV, respectively. Anharmonicities in the vibrational motion can be qualitatively taken into account by allowing the degenerate multiplets predicted by the model to be split. Candidates for all the quadrupole three-phonon states and at least four of the five quadrupole-octupole two-phonon states are observed in the data.

Experimental $B(E2)$ ratios are compared with the predictions of the vibrational model in Table V. Anharmonicities in the vibrational motion will be manifested by the occurrence of multiphonon $E2$ transitions which are strictly forbidden in the model. From the ratios listed in Table V, two-phonon transitions are hindered at least by a factor of 22 compared to one-phonon transitions, while the one three-phonon transition which was observed is hindered by a factor of ~1600. Ratios of one-phonon transitions do not show such large hindrances and are in reasonable agreement with the model predictions.

Two-phonon $E0$ transitions are permitted by the

TABLE V. Comparison of experimental $B(E2)$ ratios with the predictions of models discussed in the text.

Initial level[a] E, N, J^π	Final levels[b] $[E, \Delta N, J^\pi]_1/[E, \Delta N, J^\pi]_2$	Exp.	Vibrational model[c]	Phenomenological model[d]	Microscopic model[e] I	Microscopic model[e] II
1430, 2, (2)$^+$	[0, 2, 0$^+$]/[638, 1, 2$^+$]	0.026(2)	0.0	0.028	0.14	0.31
1955, 3, 2$^+$	[0, 3, 0$^+$]/[1207, 1, 0$^+$]	0.0006(3)	0.0	0.0012	0.32	0.067
	[638, 2, 2$^+$]/[1207, 1, 0$^+$]	0.045(9)	0.0	0.026	1.03	0.48
	[1430, 1, (2)$^+$]/[1207, 1, 0$^+$]	7(1)	0.41	0.64	6.99	
1988, 3, (3$^+$, 4$^+$)[f]	[638, 2, 2$^+$]/[1430, 1, (2)$^+$]	0.04(1)	0.0	0.038	0.024	0.17
	[1288, 1, 4$^+$]/[1430, 1, (2)$^+$]	0.29(4)	0.40	0.66	0.16	0.13
2080, 3, (3$^+$, 4$^+$)[g]	[638, 2, 2$^+$]/[1430, 1, (2)$^+$]	0.005(3)	0.0	0.0028	1.06	0.068
	[1288, 1, 4$^+$]/[1430, 1, (2)$^+$]	0.33(22)	0.91	0.46	0.82	0.18

[a] N is the number of phonons assigned to the level in the vibrational model.
[b] ΔN is the change in phonon number for a transition.
[c] Reference 31.
[d] Reference 19.
[e] Reference 20. Columns labeled I and II represent different ways of correlating calculated levels with experimental levels. See text for details.
[f] Theoretical values are calculated assuming state is 4$^+$ except for column labeled II where 3$^+$ is assumed.
[g] Theoretical values calculated assuming state is 3$^+$ except for column labeled II where 4$^+$ is assumed.

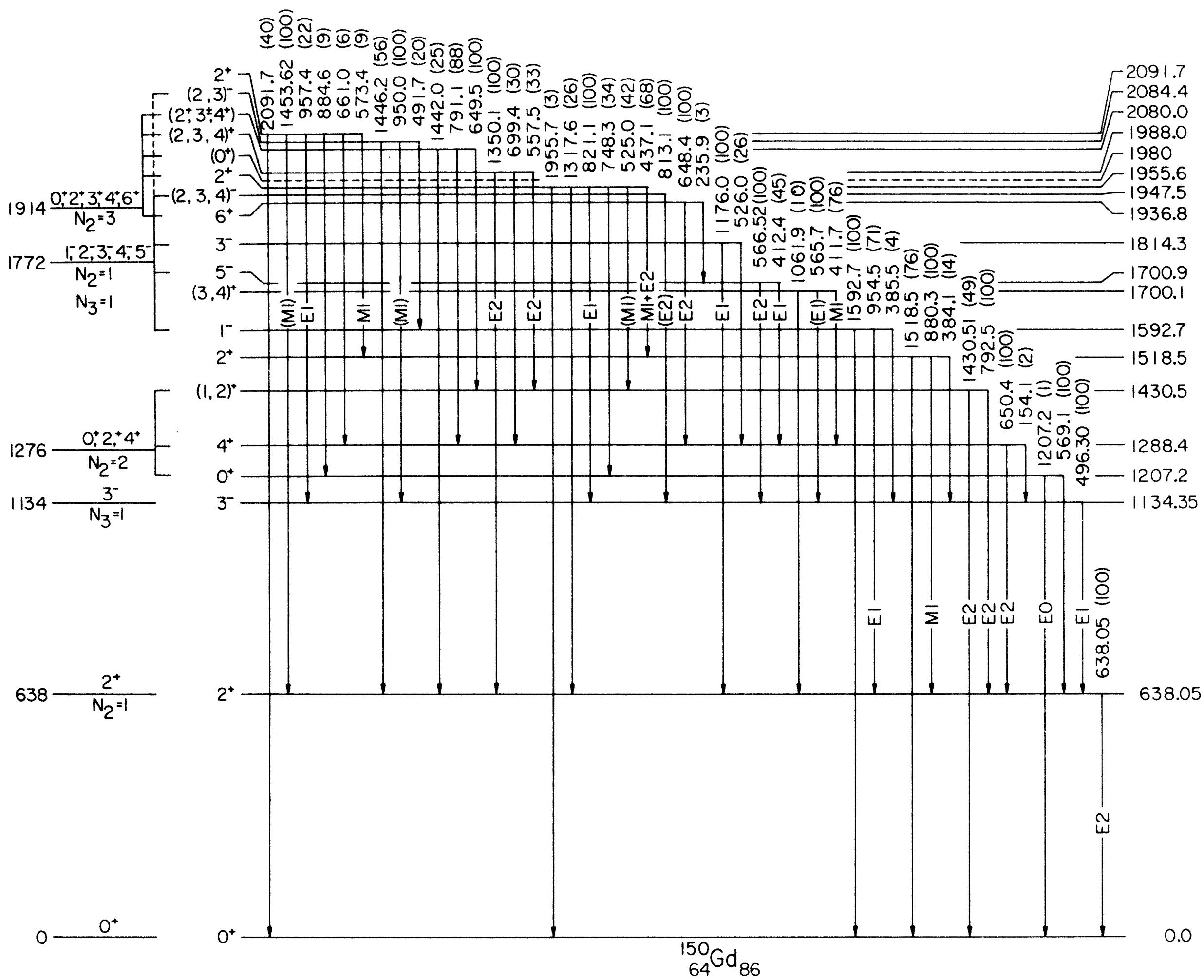

FIG. 2. Low-lying levels in ^{150}Gd. In addition to the results from the present study, data from Refs. 4, 9–11, and 15 have been included. The relative transition intensity for branching out of each level is given in parentheses. A possible correspondence with the predictions of the vibrational model is indicated on the left.

vibrational model. The experimental value of the X parameter $[B(E0)/B(E2)]$ for the 1207.2-keV level is 0.020(3). The predicted value is 0.023. The theoretical X value, however, is only an estimate based on the experimental $B(E2; 2^+ \rightarrow 0^+)$ for ^{148}Sm (Ref. 32). The corresponding value for ^{150}Gd has not been measured.

The vibrational model describes the low-lying states in ^{150}Gd surprisingly well, especially when allowances are made for anharmonic effects in the vibrational motion. This vibrational description does not, however, account for two of the experimental levels below 2 MeV. These levels at 1518.5 and 1700.3 keV occur at an energy which is intermediate between the quadrupole two- and three-phonon states.

The 1518.5-keV 2^+ level is only 88 keV above the 2^+ level at 1430.5 keV which is assigned as the two-phonon state. The assignment is based on the deexcitation characteristics of these levels to the 638.05-keV 2^+ level. The 880.3-keV transition (1518.5 → 638.05) is predominantly $M1$ ($\delta_{E2/M1}^2 < 0.5$) while the 792.3-keV transition (1430.5 → 638.05) is mostly $E2$ ($\delta_{E2/M1}^2 > 15$). These limiting values of mixing ratios have been estimated from the α_K values in Table II. Since $M1$ transitions are forbidden in the vibrational model, the 1430.5-keV level is regarded as the more likely candidate to be a vibrational state. From the available data it is not possible to assign a particular structure of the 1518.5-keV level. The multipolarity of the 880.3-keV transition, however, suggests that it has a large admixture of quasiparticle components. A collective model would not be expected to account for such a state.

The 411.7-keV transition which depopulates the 1700.3-keV $(3,4)^+$ level to the 1288.4-keV 4^+ level also has a large $M1$ component ($\delta_{E2/M1}{}^2 < 1.8$). A large error is associated with our value of α_K for the 411.7-keV transition. If the data of Vylov *et al.*[5,6] are used, $\delta_{E2/M1}{}^2$ is < 0.57. The $M1$ component in the 411.7-keV transition suggests that the 1700.3-keV level also has a large admixture of quasiparticle components. Furthermore the γ decay patterns for the 1518.5- and 1700.3-keV levels are similar as can be seen in Fig. 2. Transition probabilities are summarized in Table VI. If these levels were decaying without preference to the various final states, then the experimental values of $B(E1)/B(E2)$ and $B(M1)/B(E2)$ ratios in Table VI should approach the values for single-particle transition probabilities. These single-particle ratios are listed in Table VI for comparison.

Low-lying quasiparticle states have been proposed to explain the extra 0^+ and 2^+ states found in in the vibrational Cd isotopes.[33] These extra states are also at an energy between the quadrupole two- and three-phonon states. The transitions from the vibrational and quasiparticle 2^+ states to the first 2^+ state in ^{114}Cd, for example, are similar to the 792.3- and 880.3-keV transitions in ^{150}Gd in that they have $\delta_{E2/M1}{}^2$ values of 1.96 and 0.0025, respectively.[34]

For the purposes of the following discussions we shall assume that the 1518.5- and 1700.3-keV levels are quasiparticle states of an unspecified structure and that they are relatively unmixed with nearby vibrational states.

B. Systematics

Level schemes of the even-even Gd isotopes with 82 to 94 neutrons are shown in Fig. 3. To facilitate comparisons the levels have been arranged in Sakai's quasirotational band representation.[43] Only the ground state, β, γ, and $K = 0^-$ octupole quasibands are shown. In the present discussion it is convenient to make no distinction between rotational and quasirotational bands.

The effect of adding pairs of neutrons above the 82-neutron closed shell is seen in Fig. 3. Low-lying levels in the single-closed-shell nucleus ^{146}Gd have been described in terms of quasiproton excitations.[35] The quasiground band in ^{148}Gd is similar to that in ^{146}Gd in that the spacing of the levels decreases with spin. In other 84-neutron nuclei such structure has been attributed to the coupling of two $2f_{7/2}$ neutrons to an 82-neutron core.[44] The addition of two more neutrons produces the vibrational ^{150}Gd. A spherical-to-prolate shape transition occurs between six and eight neutrons beyond the closed shell. Both ^{152}Gd and ^{154}Gd can be considered to be transitional, the former being spherical but easily deformed while the latter is weakly deformed but soft to β and γ vibrations. The Gd isotopes with more than 90 neutrons have level schemes characteristic of stably deformed nuclei.

TABLE VI. $B(E1)/B(E2)$ and $B(M1)/B(E2)$ ratios for the deexcitation of the 1518.5- and 1700.3-keV levels compared with single-particle values.

Level energy (keV)	$B(E1)/B(E2)$ (fm^{-2})	$B(M1)/B(E2)$ $\left[\left(\frac{e\hbar}{2Mc}\right)^2 / e^2\,\text{fm}^4\right]$
1518.5	$2.1(2)\times10^{-5}$	$1.1(1)\times10^{-3}$
1700.3	$6(3)\times10^{-5}$	$1.0(5)\times10^{-2}$
Single particle	7.2×10^{-3}	3.8×10^{-2}

The quasibands in ^{150}Gd appear to be a systematic extension of bands found in the heavier Gd isotopes. The spacing of the states in each of the bands shows a progression from rotational to vibrational values as the shape transition region is crossed. Even the odd-even staggering of states in the quasi-γ band in ^{152}Gd is preserved in ^{150}Gd.

The quasi-β and quasi-γ bandhead energies also follow predictable trends. They are at a minimum in the soft transitional nuclei and increase in energy as the isotopes take on more rigid spherical or spheroidal shapes. A drop in energy of the one-phonon octupole vibrational state (3^- member of the quasioctupole band) has been noted in the spherical nuclei above 82 neutrons. This has been correlated with the availability of negative-parity states $\nu(f_{7/2}i_{13/2})$ at relatively low excitation energies.[45]

The trends observed in these Gd isotopes are reasonably well understood and clearly show the systematics of the 88- to 90-neutron shape transition. It would be interesting to compare the adding of neutrons above the 82-neutron closed shell with the corresponding proton case. The quasiground band levels in ^{204}Po (Ref. 46) and ^{206}Rn (Ref. 47) show a spacing which is indicative of coupling $2h_{9/2}$ protons to a core.

In Fig. 4 the level schemes of the even-even 86-neutron isotones are compared with that for ^{150}Gd.

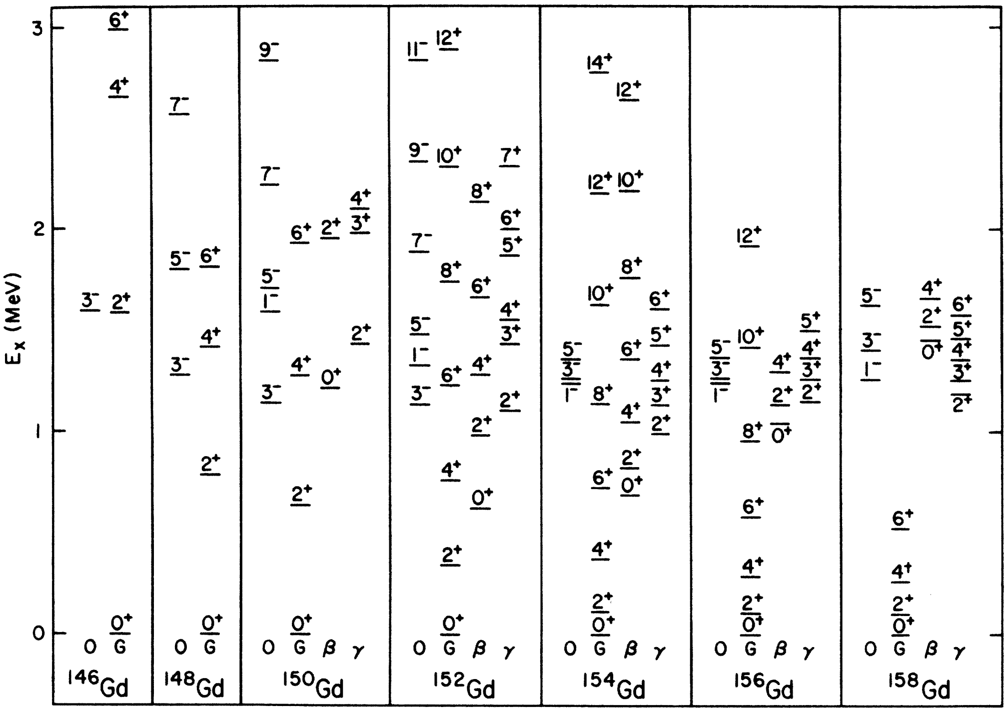

FIG. 3. Quasirotational bands in the even-even Gd isotopes. The quasigroundstate (G), quasi-β, quasi-γ, and $K=0^-$ quasioctupole (O) bands are shown. In addition to the results of the present study, data are also taken from Refs. 35, 36 (^{146}Gd); 37 (^{148}Gd); 4, 15 (^{150}Gd); 22, 38 (^{152}Gd); 39, 40 (^{154}Gd); 41 (^{156}Gd); and 42 (^{158}Gd).

Most of these nuclei have not been studied in detail; thus comparisons can be made for only a few levels.

The energy of the first 2^+ state is at a maximum in ^{150}Gd while the energy of the first-excited 0^+ state (quasi-β bandhead) drops ~0.5 MeV from ^{146}Nd to ^{150}Gd. The energy of the second 2^+ state (quasi-γ bandhead) remains approximately constant. The first excited 4^+ and 6^+ states follow the trends of the first 2^+ state.

From a survey of positive-parity two-phonon states in even-even nuclei from Zn to Te, Hadermann and Rester[52] suggest that a drop in the two-phonon 0^+ energy coupled with a rise in the one-phonon 2^+ energy can be correlated with the filling of spherical proton or neutron orbitals. There is some evidence from α-decay studies[53] that the spherical 64-proton nuclei have an extra stability which could be associated with the filling of the $1g_{7/2}$ and $2d_{5/2}$ proton orbitals. The systematics of the positive-parity states in the 86-neutron isotones appear to provide further evidence of orbital filling at 64 protons.

The systematics of the negative-parity states may also be understood in the same way. The en-

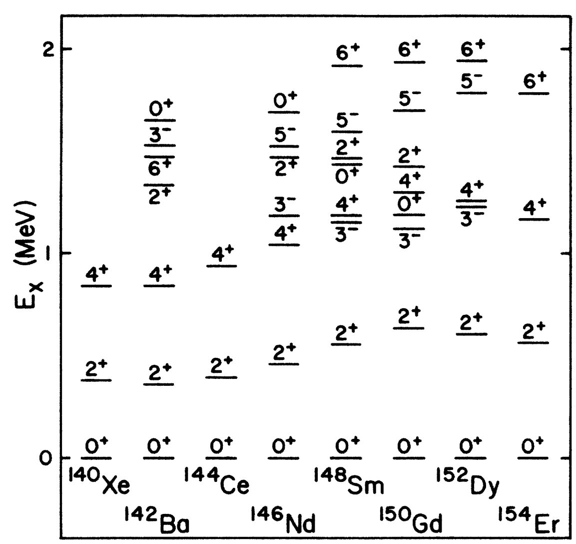

FIG. 4. Level schemes of the even-even 86-neutron isotones from Xe to Er. In addition to the results of the present study, data are also taken from Refs. 48 (^{140}Xe, ^{144}Ce); 43 (^{142}Ba); 36 (^{146}Nd); 49 (^{148}Sm); 4, 15 (^{150}Gd); 50 (^{152}Dy); and 51 (^{154}Er).

ergy of the first 3^- state also reaches a minimum at ^{150}Gd. A similar trend has been noticed in the 82- and 84-neutron isotones and ascribed to the lowering in energy of the $\pi(d_{5/2}h_{11/2})$ and $\pi(g_{7/2}h_{11/2})$ states as the spherical $1g_{7/2}$ and $2d_{5/2}$ orbitals are filled.[45] The spacing of the 5^- level above the 3^- level suggests that it is possibly a quadrupole-octupole two-phonon vibration.

It is obvious from Fig. 4 that not all the 86-neutron isotones are examples of vibrational nuclei. From Xe to Nd the isotones exhibit a more transitional character as evidenced by the relatively high energies of the quasi-β and quasi-γ bandheads with respect to the 4^+ member of the ground band. The data for ^{154}Er suggest a return to a more transitional character in the heavier isotones. Wilhelmy *et al.*[48] have drawn a similar conclusion from the analysis of energy ratios of the first 4^+ and 2^+ states for nuclei in this region. The best candidates for vibrational nuclei among the 86-neutron isotones appear to be those nearest the orbital closure at 64 protons. It would be interesting to see whether ^{148}Sm and ^{152}Dy can be described within a vibrational framework.

C. Comparison with theory

1. Phenomenological model

The experimental data for ^{150}Gd have already been compared with the predictions of the phenomenological vibrational model. The agreement was remarkably good considering the simplicity of this model. For a more quantitative description of the data a phenomenological model which includes anharmonicity in the vibrational motion is required.

One such model for quadrupole collective motion is based on a Hamiltonian for an anharmonic quadrupole oscillator. All terms are kept which do not violate time reversal or rotational invariance. Gneuss and Greiner[19] have described this model in detail and demonstrated that it is capable of reproducing collective level spectra in a wide variety of nuclei. For the calculation performed here, the Hamiltonian contained only five free parameters, since the potential energy terms above fourth order were not used. In all other respects the calculation is equivalent to the one described by Gneuss and Greiner.

The experimental levels in ^{150}Gd and those predicted by this model are compared in Fig. 5. The parameters P_2, P_3, C_2, C_3, and C_4 [see Eq. (2), Ref. 19] for this calculation were 0.00487, 0.0193, 16.62, 32.55, and 91.38 MeV, respectively. These parameters were not determined from a least-squares fit to the data. Undoubtedly better results could be obtained if such a procedure were used.

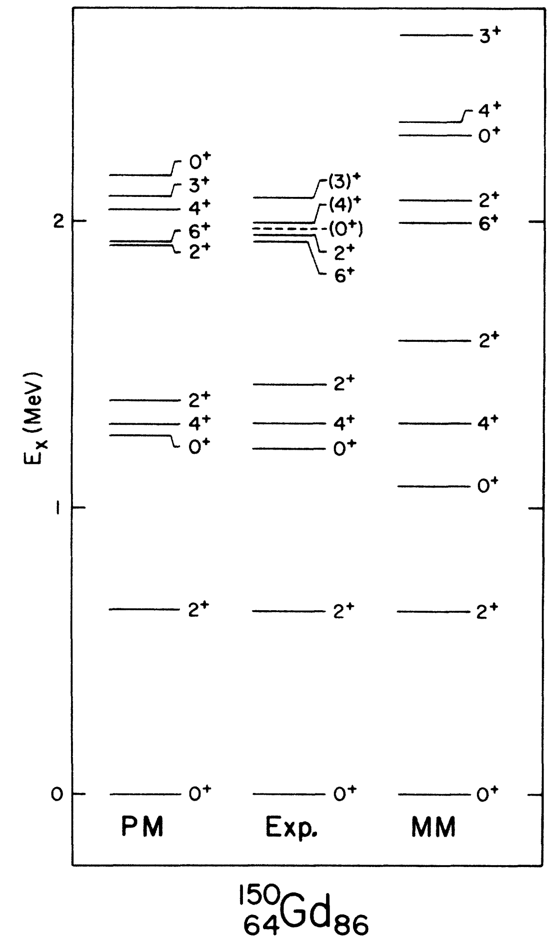

FIG. 5. Comparison of the experimental levels in ^{150}Gd with those predicted by the phenomenological model (PM) of Gneuss and Greiner and the microscopic model (MM) of Kishimoto and Tamura.

The calculation reproduces all but the three-phonon 0^+ state reasonably well.

An ambiguity exists in attempting to correlate the experimental and theoretical results since the J^π values for the 1988.0- and 2080.0-keV levels are not uniquely determined. The calculation indicates that they should be 4^+ and 3^+, respectively, while the systematics discussed above suggests the opposite ordering. Unfortunately, either ordering is permitted by the currently available data. Until this question can be experimentally resolved, the J^π values for these states will be assumed to be those which are most consistent with what is being compared. This ambiguity also exists in comparisons with the microscopic model in the next section.

Transition probabilities were calculated under the assumption that the $B(E2; 2^+ \rightarrow 0^+)$ value for ^{150}Gd is the same as that for ^{148}Sm (Ref. 32). Experimental and calculated $B(E2)$ ratios are shown in Table V. The agreement is good. Except for one value all the calculated ratios are within a factor of 2.3 or less of the experimental ratios.

2. *Microscopic model*

Two different microscopic models have been used to describe the 88- to 90-neutron shape transition in the Sm isotopes. Kumar and Baranger[54,55] employ the microscopic pairing-plus-quadrupole model to determine the parameters of Bohr's collective Hamiltonian. Kishimoto and Tamura[20] start with a fermion Hamiltonian having monopole pairing, quadrupole pairing, and quadrupole particle-hole residual interactions. The parameters for a collective boson Hamiltonian are obtained through the use of boson-expansion techniques. A major difference in the two models results from the way in which the coupling to noncollective modes of excitation is treated. Kumar and Baranger adopt the adiabatic assumption while Kishimoto and Tamura include this coupling in an approximate way. Since the effects of this coupling should be important in describing vibrational nuclei, the boson-expansion model may be more appropriate for ^{150}Gd.

The calculation which has been made is essentially the same as that described in detail in Ref. 20. The two adjustable parameters of the model representing the strengths of the quadrupole pairing and quadrupole particle-hole interactions were taken to be 0.65 and 0.765, respectively, in units of $240A^{-5/3}$ MeV. The parameters were chosen to reproduce the energies of the first 2^+ and 4^+ states in ^{150}Gd.

The calculated results may be compared with experiment in two ways. In the first method the correspondence between calculated and experimental levels is based on energies, spins, and parities. For example, the 2_3^+ state observed at 1955.6 keV is to be compared with the 2_3^+ state calculated to occur at 2200 keV. This is shown in Fig. 5. The experimental spin sequence is reproduced if the 1988.0- and 2080.0-keV levels are assumed to be 4^+ and 3^+, respectively. The average deviation of the experimental and theoretical levels is ~190 keV. For the phenomenological model the average deviation was ~30 keV. Calculated $B(E2)$ ratios for this method of correlating the calculated and experimental results are given in Table V in the column labeled I. The agreement is relatively poor.

Alternatively the calculated and experimental results can be compared on the basis of quasirotational bands. The grouping of states into bands is based on $B(E2)$ values and values of static quad-

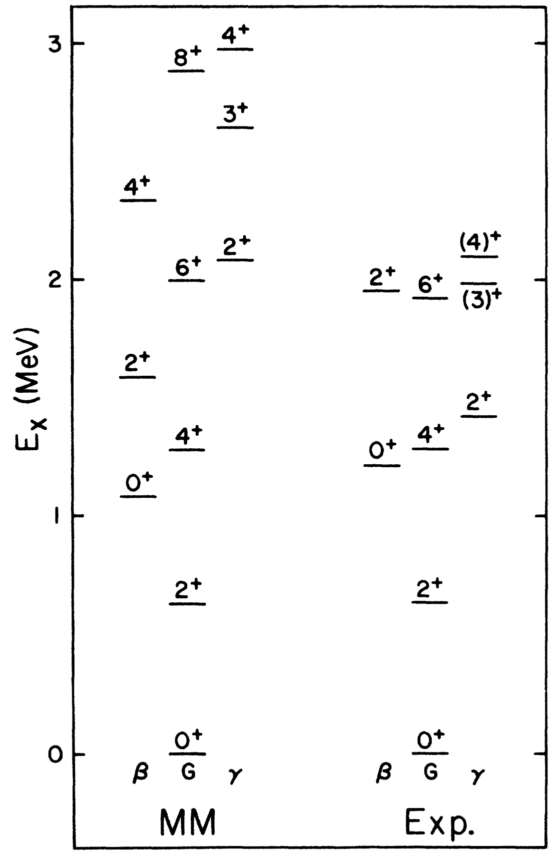

FIG. 6. Comparison of experimental quasirotational bands for ^{150}Gd with those predicted by the microscopic model (MM) of Kishimoto and Tamura.

rupole moments.[20] In this case the 2_3^+ state at 1955.6 keV is to be compared with the calculated 2^+ state at 1600 keV which is a member of the quasi-β band. Energy spectra are shown in Fig. 6 for this representation and in Table V for $B(E2)$ ratios (column labeled II). In this case, the 1988.0- and 2080.0-keV levels are assumed to be 3^+ and 4^+, respectively. The calculated quasi-β band is found to be too low in energy while the quasi-γ band lies too high. The spacing of the states within each band is reasonably consistent with experiment and there is even a slight odd-even bunching of the quasi-γ band states. However, the calculated $B(E2)$ ratios again do not reproduce the data very well.

The boson-expansion model does not satisfactorily reproduce either the experimental level spectrum or $B(E2)$ ratios. The model predicts ^{150}Gd to be more transitional than the data would imply. This is observed in three ways. First, if one compares the relative positions of the excited quasibands with respect to the quasiground band states,

TABLE VII. Experimental $B(E2)$ ratios for ^{150,152,154}Gd and predictions of the microscopic boson-expansion model for ^{150}Gd.

Initial level [a]	Final levels [a]	^{150}Gd	^{152}Gd [b]	^{154}Gd [c]	Theo.
2_β	$0_g/2_g$	0.013(6)	0.0192(19)	0.121(4)	0.139
	$4_g/2_g$		2.04(27)	2.72(8)	1.78
	$0_\beta/0_g$	1670(840)	107(11)	125(6)	15.0
4_β	$2_g/4_g$			0.0855(25)	0.148
	$6_g/4_g$			5.91(18)	2.45
2_γ	$0_g/2_g$	0.026(2)	0.142(14)	0.464(11)	0.307
	$4_g/2_g$			0.145(5)	1.74
3_γ	$2_g/4_g$	0.14(4)	0.45(5)	1.032(31)	1.28
	$2_\gamma/2_g$	25(6)	<28	16.5(8)	5.83
4_γ	$2_g/4_g$	0.015(10)	0.071(15)	0.138(7)	0.377
	$2_\gamma/2_g$	200(120)	48(21)		14.8

[a] Experimental levels are labeled by their quasirotational band assignments.
[b] Reference 22.
[c] References 22 and 39.

then the calculated spectrum for ^{150}Gd resembles the experimental spectrum for the transitional nucleus ^{152}Gd (see Fig. 3). Second, in Table VII, experimental $B(E2)$ ratios for ^{150,152,154}Gd are compared with the model predictions. Many of the ratios calculated for ^{150}Gd are more consistent with the experimental values for the transitional nuclei (particularly ^{154}Gd) than with those for ^{150}Gd. Third, the potential wells from the phenomenological and microscopic calculations are compared in Fig. 7. To make this comparison more meaningful, the Hamiltonian for each model has been transformed so that all anharmonicities are included only in the potential energy terms. A prescription for this canonical transformation is given in Appendix I of Ref. 20. One would expect that the potential well for a vibrational nucleus would be centered around $\beta=0$. While neither well exhibits this property, the well for the phenomenological model is less asymmetric about $\beta=0$ than the microscopically calculated well.

These comparisons do not make clear whether a basic problem exists with the boson-expansion model or whether the problem lies in some of the "fixed" parameters (e.g., single-particle energies). In order to describe the level scheme for ^{150}Gd with a microscopic model it may be vital to include the effects of the extra states at 1518.5 and 1700.3 keV. At present such a model is not available. Kishimoto and Tamura have indicated that noncollective states may be explicitly included within the framework of the boson-expansion model and some preliminary results from such a calculation have been reported.[33] It would be very interesting to see if this model could reproduce the experimental data for ^{150}Gd.

3. *Negative-parity states*

Theoretical models for describing the negative-parity states resulting from the coupling of quadrupole and octupole vibrations are not well developed. One reason for this lies in the fact that such models must first adequately describe the quadrupole collective states before treatments of octupole vibrations or the quadrupole-octupole

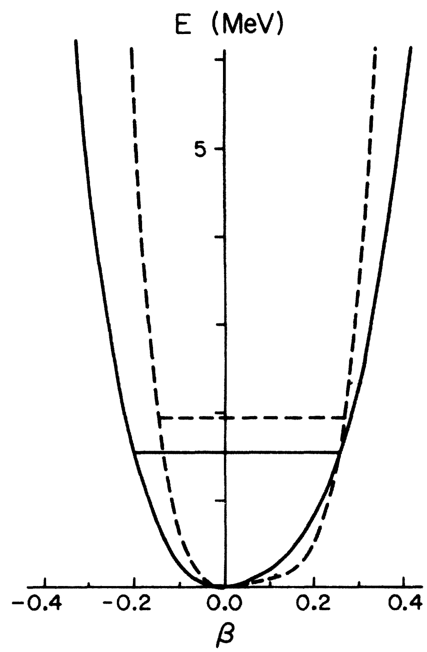

FIG. 7. Potential wells from the phenomenological (solid line) and microscopic (dashed line) models for ^{150}Gd.

coupling can be trusted. Furthermore not much experimental data are available for such states.

Vogel and Kocbach[56] have developed a microscopic model for calculating the two-phonon states resulting from the coupling of one quadrupole and one octupole vibration. Basically this model uses techniques similar to those developed by Kumar and Baranger[54,55] for describing quadrupole collective states. Numerical results have been reported for ^{146}Nd and ^{148}Sm. In general the energies of the calculated levels were too high. This was attributed in part to an inadequate treatment of the quadrupole motion in the model.

Calculations for the negative-parity states in ^{150}Gd will not be presented here. A comparison of the experimental data with the predictions of a phenomenological quadrupole-octupole coupling model[38] can be found in a discussion of the (α, xn) reaction[15] in which negative-parity states are populated to much higher spins.

V. CONCLUSIONS

The decay of 3.6-h ^{150}Tb is found to populate a large number of low-spin levels in ^{150}Gd. The levels below ~2 MeV have properties which strongly resemble those expected for a vibrational nucleus. Two of the low-lying levels which are not accounted for as vibrational states may have large admixtures of quasiparticle components. The proposed vibrational levels in ^{150}Gd can be reproduced with the phenomenological model of Gneuss and Greiner[19] but the microscopic boson-expansion model of Kishimoto and Tamura[20] predicts ^{150}Gd to be more transitional than the data indicate.

The vibrational interpretation of the levels in ^{150}Gd fits well into the systematics of the 88- to 90-neutron region in the Gd isotopes. The systematics of the known 86-neutron isotones are found to be influenced by the closure of the spherical $g_{7/2}$ and $d_{5/2}$ proton orbitals at $Z=64$. The isotones near the orbital closure are vibrational while those farther away are more transitional.

ACKNOWLEDGMENTS

We thank T. Kishimoto for his help in interpreting the experimental results and for supplying the computer codes for the theoretical calculations. We acknowledge valuable discussions with T. Tamura, P. K. Bindal, A. Ikeda, and M. Nomura. W. W. Bowman, D. R. Zolnowski, Y. Gono, M. Devous, and M. B. Hughes assisted with various aspects of data acquisition and reduction. While this work was in progress one of us (DRH) received support in the form of an NSF traineeship from the National Science Foundation and a Phillips fellowship award from the Phillips Petroleum Company.

---

†Supported in part by the U. S. ERDA and the Robert A. Welch Foundation.

*Present address: KFA Jülich, 517 Jülich, West Germany.

[1]K. Kumar and M. Baranger, Nucl. Phys. A110, 529 (1968).

[2]U. Mosel and W. Greiner, Z. Phys. 217, 256 (1968).

[3]U. Götz, H. C. Pauli, K. Alder, and H. Junker, Nucl. Phys. A192, 1 (1972).

[4]D. R. Haenni, T. T. Sugihara, and W. W. Bowman, Phys. Rev. C 5, 1113 (1972).

[5]Ts. Vylov, K. Ya. Gromov, I. I. Gromova, G. I. Iskhakov, V. V. Kuznetsov, M. Ya. Kuznetsova, A. V. Potempa, and M. I. Fominykh, Izv. Akad. Nauk SSSR Ser. Fiz. 37, 43 (1973) [Bull. Acad. Sci. USSR Phys. Ser. 37, 36 (1973)].

[6]Ts. Vylov, K. Ya. Gromov, I. I. Gromova, G. I. Iskhakov, V. V. Kuznetsov, M. Ya. Kuznetsova, A. V. Potempa, and M. I. Fominykh, Izv. Akad. Nauk SSSR Ser Fiz. 37, 48 (1973) [Bull. Acad. Sci. USSR Phys. Ser. 37, 41 (1973)].

[7]R. Arlt, H. Bayer, V. V. Kuznetsov, W. Neubert, A. A. Potemysa, W. Hagemann, and E. Herrmann, Izv. Akad. Nauk SSSR Ser. Fiz. 35, 1612 (1971) [Bull. Acad. Sci. USSR Phys. Ser. 35, 1470 (1972)].

[8]R. Arlt, V. V. Kuznetsov, W. Neubert, L. K. Peker, A. V. Potempa, and U. Hagemann, Izv. Akad. Nauk SSSR Ser. Fiz. 36, 2074 (1972) [Bull. Acad. Sci. USSR Phys. Ser. 36, 1826 (1973)].

[9]D. G. Fleming, C. Günther, G. B. Hagemann, B. Herskind, and P. O. Tjøm, Phys. Rev. Lett. 27, 1235 (1971).

[10]D. G. Fleming, C. Günther, G. Hagemann, B. Herskind, and P. O. Tjøm, Phys. Rev. C 8, 806 (1973).

[11]Th. W. Elze, J. S. Boyno, and J. R. Huizenga, Nucl. Phys. A187, 473 (1972).

[12]H. Ejiri, M. Ishihara, M. Sakai, K. Katori, and T. Inamura, J. Phys. Soc. Jpn. 24, 1189 (1968).

[13]D. Kewley, D. A. Eastham, P. D. Forsyth, B. W. Renwick, D. G. E. Martin, C. J. Gibbins, and B. Byrne, Nucl. Phys. A165, 56 (1971).

[14]K. Krien, F. Djadali, R. A. Naumann, H. Hübel, and E. H. Spejewski, Phys. Rev. C 7, 2484 (1973).

[15]D. R. Haenni and T. T. Sugihara (unpublished).

[16]K. Wilsky, K. Ya. Gromov, Zh. T. Zhelev, V. V. Kuznetsov, G. Muziol, O. B. Nielsen, and O. Skilbreid, Izv. Akad. Nauk SSSR Ser. Fiz. 32, 187 (1968) [Bull. Acad. Sci. USSR Phys. Ser. 32, 169 (1969)].

[17]Y. Gono, T. Araki, and K. Hiruta, J. Phys. Soc. Jpn. 29, 1379 (1970).

[18]C. M. Baglin, Nucl. Data Sheets 18, 223 (1976).

[19]G. Gneuss and W. Greiner, Nucl. Phys. A171, 449 (1971).

[20]T. Kishimoto and T. Tamura, Nucl. Phys. A270, 317 (1976).

[21]K. Vilskii, V. V. Kuznetsov, O. B. Nielssen, O. Skilbreid, and V. A. Khalkin, Yad. Fiz. 6, 672 (1967) [Sov. J. Nucl. Phys. 6, 488 (1968)].

[22]D. R. Zolnowski, E. G. Funk, and J. W. Mihelich, Nucl. Phys. A177, 513 (1971).

[23]J. T. Routti and S. G. Prussin, Nucl. Instrum. Methods 72, 125 (1969).
[24]D. R. Haenni, U. S. ERDA Report No. ORO-4322-18, 1976 (unpublished).
[25]D. R. Zolnowski and T. T. Sugihara, Nucl. Instrum. Methods 114, 341 (1974).
[26]Y. Gono, R. L. Watson, T. T. Sugihara, and R. A. Kuebbing, Nucl. Instrum. Methods 127, 391 (1975).
[27]R. S. Hager and E. C. Seltzer, Nucl. Data A4, 1 (1968).
[28]U. Fano, *Tables for the Analysis of Beta Spectra*, U. S. National Bureau of Standards, Applied Mathematics Series No. 13 (U. S. Government Printing Office, Washington, D. C. 1952).
[29]N. B. Gove and M. J. Martin, Nucl. Data Tables 10, 205 (1971).
[30]S. Raman and N. B. Gove, Phys. Rev. C 7, 1995 (1973).
[31]See for example, J. M. Eisenberg and W. Greiner, *Nuclear Models* (North-Holland, Amsterdam/American Elsevier, New York, 1970), p. 47 ff.
[32]P. H. Stelson and L. Grodzins, Nucl. Data A1, 21 (1965).
[33]T. Tamura, T. Udagawa, and T. Kishimoto, in Proceedings of the Symposium on Nuclear Structure, Balatonfüred, Hungary, 1975 (to be published).
[34]H. J. Kim, Nucl. Data Sheets 16, 107 (1975).
[35]J. Kownacki, H. Ryde, V. O. Sergejev, and Z. Sujkowski, Nucl. Phys. A196, 498 (1972).
[36]T. W. Burrows, Nucl. Data Sheets 14, 413 (1975).
[37]W. W. Bowman, D. R. Haenni, and T. T. Sugihara, Phys. Rev. C 7, 1686 (1973).
[38]D. R. Zolnowski, T. Kishimoto, Y. Gono, and T. T. Sugihara, Phys. Lett. 55B, 453 (1975).
[39]D. C. Sousa, L. L. Riedinger, E. G. Funk, and J. W. Mihelich, Nucl. Phys. A238, 365 (1975).
[40]Y. Gono and T. T. Sugihara, Phys. Rev. C 10, 2460 (1974).
[41]T. W. Burrows, Nucl. Data Sheets 18, 553 (1976).
[42]J. K. Tuli, Nucl. Data Sheets 12, 245 (1974).
[43]M. Sakai, At. Data Nucl. Data Tables 15, 513 (1975).
[44]K. Heyde and P. J. Brussaard, Nucl. Phys. A104, 81 (1967).
[45]O. Hansen and O. Nathan, Nucl. Phys. 42, 197 (1963).
[46]H. Beuscher, D. R. Zolnowski, D. R. Haenni, and T. T. Sugihara, Phys. Rev. Lett. 36, 1128 (1976).
[47]K. K. Seth, Nucl. Data B7, 161 (1972).
[48]J. B. Wilhelmy, S. G. Thompson, R. C. Jared, and E. Cheifetz, Phys. Rev. Lett. 25, 1122 (1970).
[49]W. Oelert, J. V. Maher, D. A. Sink, and M. J. Spisak, Phys. Rev. C 12, 417 (1975).
[50]J. F. W. Jansen, Z. Sujkowski, R. J. de Meijer, D. Chmielewska, and F. Bruining, Annual Report, Kernfysisch Versneller Instituut, Groningen, Netherlands, 1974 (unpublished), p. 50.
[51]W. W. Bowman, D. R. Haenni, and T. T. Sugihara, Progress in Research Report, Cyclotron Institute, Texas A&M University, 1973 (unpublished), p. 30.
[52]J. Hadermann and A. C. Rester, Nucl. Phys. A231, 120 (1974).
[53]W.-D. Schmidt-Ott and K. S. Toth, Phys. Rev. C 13, 2574 (1976).
[54]K. Kumar and M. Baranger, Nucl. Phys. A122, 273 (1968).
[55]K. Kumar, Nucl. Phys. A231, 189 (1974).
[56]P. Vogel and L. Kocbach, Nucl. Phys. A176, 33 (1971).